Research Square

Preprints are preliminary reports that have not undergone peer review.
They should not be considered conclusive, used to inform clinical practice,
or referenced by the media as validated information.

Integrating Seismic Safety into Development Control: A Screening Approach to Setbacks and Inter-Building Separation in Siliguri, India

Arpan Paul Singh Golla
arpanpaulsingh@gmail.com

School of Planning and Architecture Vijayawada

Shankha Pratim Bhattacharya
Indian Institute of Technology Kharagpur

Sumana Gupta
Indian Institute of Technology Kharagpur

Research Article

Keywords: Rapid Visual Screening, seismic risk, debris reach, inter-building separation, setback compliance, urban resilience, municipal planning, Siliguri

Posted Date: September 15th, 2026

DOI: https://doi.org/10.21203/rs.3.rs-9836394/v1

License: This work is licensed under a Creative Commons Attribution 4.0 International License. Read Full License

Additional Declarations: No competing interests reported.

Abstract

This paper develops a municipal screening framework to assess two geometry-related seismic concerns in dense urban areas: setback adequacy against debris reach and inter-building separation against pounding risk. Using Rapid Visual Screening data from 1,106 buildings in Siliguri Municipal Corporation, India, the analysis links observable field attributes such as building height, setbacks, side clearances, typology, floor area ratio, and plinth level to debris-reach exceedance, drift-based separation screening, and a combined operational risk flag. Debris reach was estimated using a simple collapse-angle approach, while inter-building separation was evaluated through a drift-based clearance check. Results show that 68.4% of the surveyed stock exceeds debris-safe setback at $\varphi = 45°$, 21.8% has inadequate inter-building separation at $\theta = 1.0\%$, and 31.8% falls within the combined higher-risk category. Debris insufficiency is far more widespread than separation inadequacy and rises sharply with building height, whereas separation problems are concentrated where side clearance is absent or nearly absent. A risk classification model further identifies inter-building gap, plinth-to-road level, and building height as the strongest predictors of higher-risk classification. The paper contributes a method that requires only field-observable data and extends Rapid Visual Screening beyond building-level triage. It produces outputs that map directly onto existing regulatory categories of setbacks and inter-building clearance in dense, small-plot urban areas.

1 Introduction

The risk of earthquake damage in dense urban areas depends not only on the response of individual buildings to ground shaking, but also on the interaction between the neighbouring buildings. Buildings placed close to each other can become out of phase, affecting each other, and cause pounding damage to both structural and non-structural parts (Cole et al., 2012; Lin, 1996). Many organically grown Indian cities have ageing building stock with narrow setbacks, zero-gap construction, height deviations, and mixed structural systems. In cities like Delhi and Kolkata, real estate demands make adequate seismic gaps financially impractical. Post-earthquake surveys of 2001 Bhuj Earthquake or 2006 Sikkim Earthquake have documented structural pounding leading to severe wall and column distress.

Even without total collapse, falling parapets, infill panels, and cladding debris can block adjoining roads and reduce the space available for evacuation (Sediek et al., 2021). Recently there is a growing body of literature that have emphasized on debris reach and road blockage as significant concerns of seismic risk and post event recovery (Y. Hosseini et al., 2024; Yu & Gardoni, 2022).

In India, the responsibility for translating seismic safety into built form rests primarily with urban local bodies through development control regulations. These regulations prescribe setbacks, ground coverage limits, and inter-building gaps as part of the building permit process. However, the values specified in most municipal building rules are derived from planning considerations such as light, ventilation, and fire safety rather than from seismic reasoning. The result is a structural disconnect. National codes like IS 1893 establish the engineering basis for seismic design, but local development control instruments do not consistently reflect that basis in their spatial requirements. In rapidly growing cities with dense, small-plot development and mixed building stock, this gap becomes consequential. Buildings rise above the heights for which standard setbacks offer any meaningful debris clearance, and adjacent structures are constructed with no lateral reserve space at all. These conditions are not incidental. They are the cumulative product of plot subdivision, densification, and weak enforcement over decades. Addressing them requires tools that work within the planning process, not alongside it.

Most available studies focus on individual building outcomes rather than the combined hazard picture that follows an earthquake. While we can determine if a building is prone to collapse based on its capacity, ductility, and detailing, we also need to understand whether an ambulance can navigate through a street segment where a building has collapsed (Golla et al., 2020).

Municipal engineers and planners need a simple method to convert field observations into estimates of debris extension and potential road blockage (Koren & Rus, 2025). Rapid Visual Screening (RVS) is a practical starting point for a seismic assessment of the building stocks at city scale. The method is quick and consistent across variety of building typologies and uses standard indicators (FEMA 154, 2015; Kassem et al., 2021). RVS does not replace detailed engineering analysis, but it enables quick and consistent assessment across a large number of buildings (Golla et al., 2022). Further, practical building-gap checks that indicate lateral drift demand can help identify where clearance is likely to be inadequate (Lin, 1996; Liu et al., 2022). Integrating such checks into building permits would help authorities and owners identify feasible remedies. And, wherever required separation cannot be achieved, compensatory measures like façade ties, catch systems, or engineered party wall can be specified.

This paper estimates debris extension relative to available setbacks and evaluates inter-building gap adequacy, using Rapid Visual Screening as the primary data source (FEMA, 2010; Liu et al., 2022). The proposed research method for this paper is linked to three prominent gaps in the literature. Despite decades of seismic research, a persistent gap exists i.e., RVS studies generate damage scores

but rarely extend the analysis to debris obstruction or corridor accessibility. Transportation resilience studies, by contrast, model network recovery in considerable detail yet treat structural damage as an assumed input rather than something derived from field conditions (El-Maissi et al., 2023). Although seismic pounding between adjacent buildings is well studied analytically, it remains difficult for municipal engineers to translate this knowledge into simple street-level checks (Elwardany et al., 2025; Noman et al., 2016). Field documentation of pounding damage has not been translated into corridor level guidance despite its direct relevance to land use regulation (Cole et al., 2012). Finally, while machine-learning models can identify vulnerable buildings, their outputs are not sufficiently converted into metrics that local agencies can use to permit the building construction. What is needed is an approach grounded in basic physical principles, with inputs gathered from field observation and outputs that practitioners can use directly.

We have four objectives in this study. First, we estimate debris-reach from visual screening-based observations and compare that debris-reach with observed front and side setbacks. Second, we evaluate the adequacy of inter building separation based on simplified drift-based clearance check. Third, we examine which geometric and typological features are most strongly associated with buildings classified as higher risk within the screening variables. Fourth, we interpret these findings into an indicative compliance framework that relates setbacks and gaps to height and typology. This is followed by identification of compensatory measures where geometry cannot be changed.

The rest of the paper is structured as follows. Section 2 introduces the study area. Section 3 describes the methods, covering debris-reach estimation, separation adequacy evaluation, and the risk classification model. Section 4 presents result across the surveyed stock. Section 5 discusses implications for local development control under the West Bengal Municipal Building Rules, and Section 6 presents the conclusions.

2 Study Area

Siliguri Municipal Corporation (SMC) is a major urban centre in North Bengal and is located on the strategic Siliguri Corridor, that connects mainland India to the North-eastern states. The Municipal Corporation comprises of 47 wards over about 41.9 km² and functions as a regional hub for trade, logistics, health, and education. The city is located on the Mahananda floodplain at the Himalayan foothills and falls within Seismic Zone VI (revised from the earlier Seismic Zone IV) as per Indian seismic zoning framework (Fig. 1). These characteristics make Siliguri a relevant and tractable case for the analysis.

Similar to other cities, the inner city in Siliguri is characterised by denser and more compact development, while peripheral wards are relatively lower rise and less compact. The lack of building spacing, and presence of access constraints is more pronounced in the inner city. Therefore, we use ‘ward’ as the scale of the study since it is both an administrative unit and a spatial unit through which planning control is commonly carried out in Indian cities.

Of the 47 wards in the city, a total of nine wards were selected based on differential densities and heterogenous housing conditions in the city. Within the selected wards, every 10th building was surveyed systematically to avoid any bias. The survey recorded building height, front and side setbacks, structural typology, plinth level relative to road level, and basic geometric indicators. Where direct measurement was not feasible, height was estimated as 3.0 m per storey which was found to be average in the study area.

3 Methods

The methodology combines Rapid Visual Screening with two geometry-based hazard checks and a risk classification model, organised into three steps.

3.1 Debris-reach exceedance

The first analysis estimates whether building debris-reach exceeds the available setback. Debris reach was approximated using a simple collapse-angle family:

$d \approx H\tan(\phi)$ where d is debris reach, H is building height, and ϕ is the assumed collapse angle. Three angles were tested i.e., 30°, 45°, and 60° which are predominantly seen in the literature (Argyroudis et al., 2005). Exceedance was highlighted when estimated debris reach was greater than the recorded front or side setback on that frontage. This approach is simple and has been widely accepted in the literature (Ertugay et al., 2016). It does not carry out a detailed collapse modelling, but it presents a transparent screening rule that is linked directly to frontage clearance and setback review (Sediek et al., 2021; Yu & Gardoni, 2022). Exceedance rates

were then calculated by ward, height class, and structural typology. To model uncertainty in these proportions, 95 % bootstrap confidence intervals were computed using 1,000 resamples within each reportng stratum.

3.2 Inter-building separation adequacy

The second step evaluates whether available side clearance is adequate under a simplified drift-based screening rule. Required separation was estimated as:

$s_{req} = \Delta_1 + \Delta_2$ where the lateral displacement, Δ for each adjacent building is:

$\Delta = \theta H$ Here, θ is the storey-drift ratio and $H$is building height. The drift ratio was varied from 0.3% to 1.0% to cover a practical range from serviceability-level response to near-yield screening conditions in low- to mid-rise stock (Hong et al., 2003; Lin, 1996; Liu et al., 2022). The idea here is to test whether observed clearances are plausibly inadequate under auditable assumptions.

For each building, we evaluated the left and right sides independently. Where a neighbouring structure was present, side clearance was measured as the actual wall-to-wall gap. On open sides without an adjacent building, we used the recorded side setback. A side was deemed inadequate if the available clearance fell below the required separation distance $sreq$. A building was flagged as having inadequate separation if at least one of its sides did not meet the requirement. We also separately noted cases where both sides were inadequate.

3.3 Risk classification using regularised logistic regression

The third analysis uses regularised logistic regression to identify which observed variables are most strongly associated with higher-risk buildings. Logistic regression was selected because it is transparent, reproducible, and easier to audit than black-box classifiers. The model used an L2 penalty and five-fold stratified cross-validation. This combination provides stable estimates while limiting overfitting in a dataset with mixed variable types and moderate class imbalance.

The binary target classified a building as high risk when either of the following conditions was met:

1. indicative damage grade ≥ 4, or
2. joint geometric failure, defined here as debris exceedance at $\phi = 45^\circ$ or gap inadequacy at $\theta = 1.0\backslash\%$.

This target combines structural screening outcome and geometry-based screening outcome. It is therefore interpreted as an operational municipal risk flag rather than as a pure structural damage predictor.

The predictor set included building height, front setback, left setback, right setback, minimum inter-building gap, floor area ratio (FAR), structural typology, and plinth level relative to road level. Model performance was reported using cross-validated ROC AUC and F1 score. Probability calibration was then carried out using Platt scaling on the training data before evaluation on the validation split. To interpret model behaviour, permutation feature importance and partial dependence curves were used for the leading predictors.

3.4 Compliance framework and compensatory measures

The final step translates the preceding analyses into an indicative compliance framework. Minimum front setbacks are linked to debris-reach screening. Minimum side clearances and inter-building gaps are linked to the separation check. These values are organised by height class and structural typology so that the results can be read as a practical review aid rather than as a replacement for detailed engineering design. Where required geometry cannot be achieved, the framework identifies compensatory measures such as façade restraint, catch systems, or engineered party-wall details.

3.5 Sensitivity analysis

For debris reach, recalculation was performed for ϕ = 30^∘, 45^∘, and 60^∘. For separation adequacy, recalculation was performed for θ = 0.3%, 0.5%, 0.75%, and 1.0%, spanning serviceability-level response to near-yield screening conditions. The subset is dominated by low- to mid-rise buildings with a median height of 6.0 m and, therefore, the drift-induced demand is still small in absolute terms, not exceeding 0.12 m at the upper bound of the tested range. The sensitivity test was thus designed not to test for a threshold crossing, but to confirm that the classification of inadequacy is robust to the assumed level of drift and to determine whether the mechanism is clearance-driven or demand-driven. For this purpose, a clearance ratio diagnostic and a zero-gap share statistic were included as additional columns in Table 6. Height values derived from measured field observations were also compared with height values estimated from storey count where direct measurements were unavailable.

4 Results

A total of 1,106 buildings were screened using the RVS protocol. The section below covers building stock characteristics, debris-reach exceedance, separation adequacy, and the risk classification outputs.

Across the sample, the surveyed stock is predominantly low- to mid-rise, with a mean height of 2.36 storeys and a range of 1 to 14 storeys. Buildings up to 6 m account for 58.9% of the sample, while only 0.8% exceed 15 m (Table 1).

Table 1
Height distribution across the surveyed buildings

Height class	Count	Share %
≤ 6 m (1–2 storeys)	651	58.9
6–9 m (3 storeys)	233	21.1
9–12 m (4 storeys)	170	15.4
12–15 m (5 storeys)	42	3.8
> 15 m (6 + storeys)	9	0.8

Table 2
Share of surveyed buildings with VI and PI

Metric	Count	Share %
Vertical Irregularity present	639	62.6
Plan/Horizontal Irregularity present	568	54.6
Both VI & PI	334	33.4
Neither	188	18.8

Average front setback is 2.15 m, and average side setback lies between 1.35 m and 1.38 m. At the same time, 23.3% of buildings have at least one zero setback, indicating that a substantial share of the stock has no lateral reserve space at one edge. Vertical irregularity is present in 62.6% of buildings, plan irregularity in 54.6%, and both forms together in 33.4% (Table 2). The structural hazard classes are dominated by C3 buildings (58.1%), followed by U3 (18.4%), C1 (11.6%), and C2 (5.1%). The mean collapse probability is 17.47%, and 36.2% of buildings exceed a 10% collapse probability threshold. Taken together, these figures indicate that the surveyed stock is not only dense, but also geometrically and structurally uneven in ways that matter for debris spill over and interaction effects.

4.1 Debris Exceedance Analysis

Debris exceedance was evaluated for the subset of buildings with collapse probability $P \geq 0.30\,(n = 174)$ using the collapse-angle family $d \approx H\tan(\phi)$, with $\phi = 30^\circ, 45^\circ$, and 60°. Exceedance was recorded when the estimated debris reach on a side was greater than the measured side setback on that side. Table 3 reports left-side, right-side, either-side, and both-side exceedance rates for the full subset. Even under the most conservative assumption $(\phi = 30^\circ)$, 92.5% of buildings exceed setback on at least one side. This rises to 98.9% at $\phi = 45^\circ$ and 100% at $\phi = 60^\circ$. Both-side exceedance is also high, increasing from 83.9% at 30° to 92.5% at 45° and 99.4% at 60°. These results show that debris-safe lateral clearance is uncommon within the higher-probability subset and that this conclusion is robust across the tested angle band.

Table 3
Overall exceedance (all wards)

ϕ (deg)	N (P ≥ 0.3)	Exceed L (n)	Exceed L (%)	Exceed R (n)	Exceed R (%)	Exceed Either (n)	Exceed Either (%)	Exceed Both (n)	Exceed Both (%)
30	174	151	86.8	156	89.7	161	92.5	146	83.9
45	174	166	95.4	167	96.0	172	98.9	161	92.5
60	174	174	100.0	173	99.4	174	100.0	173	99.4

The ward-wise pattern, shown in the corresponding figure and table, indicates that exceedance is widespread rather than isolated. The most exposed wards are those where either-side exceedance approaches or reaches 100% at $\phi = 45^{\circ}$. The important result here is not the exact ranking of wards, but the consistency of the pattern: once buildings enter the higher-probability subset, setback insufficiency becomes the norm rather than the exception. Debris-reach screening is therefore a practical frontage-level indicator for municipal review.

Building on the debris-reach results, the study also examined ground coverage and footprint compliance with the West Bengal Municipal (Building) Rules, 2007. Because rear setbacks were not recorded, two scenarios were tested: Scenario A, where rear setback was taken as zero, and Scenario B, where rear setback was assumed equal to the front setback. Scenario B is used as the primary reporting basis. Under this assumption, median ground coverage is 0.588 and 39.5% of buildings are non-compliant. Under Scenario A, median ground coverage rises to 0.714 and non-compliance increases to 64.0%. Ward-level results are reported in Table 4, and plot-area compliance is reported in Table 5.

Table 4
Ward-wise patterns (Scenario B)

Ward	n	Median GC	Non-compliant (%)	Median D: W
2	176	0.594	41.5	0.54
4	237	0.595	44.3	0.61
5	178	0.575	34.8	0.58
22	140	0.513	23.6	0.55
29	153	0.629	47.7	0.57
42	218	0.600	40.8	0.50

Table 5
Overall compliance by plot area (Residential limit)

Plot area band	N	Compliant — Scenario B	Non-compliant — Scenario B
≤ 200 m²	826	532 (64.4%)	294 (35.6%)
201–500 m²	237	117 (49.4%)	120 (50.6%)
> 500 m²	39	18 (46.2%)	21 (53.8%)

Compliance declines with increasing plot size, from 64.4% on plots up to 200 m² to 49.4% for 201–500 m² plots and 46.2% for plots above 500 m². The median plan depth-to-width ratio under Scenario B is 0.56, indicating that many buildings are relatively shallow and wide in plan. In combination with narrow side setbacks, such forms reduce the available space for debris containment and increase exposure to contact and spillover effects.

4.2 Adequacy of Inter-Building Separation Against Drift-Based Targets

Inter-building separation was evaluated for the same subset of buildings with $P \geq 0.30\,(n = 174)$. Required separation was estimated as $s_{req} = \Delta_1 + \Delta_2$, where $\Delta = \theta H$, and θ was varied from 0.3 percent to 1.0 percent and the results are as shown in Table 6.

Table 6
Overall separation inadequacy for buildings with a collapse probability greater than 0.3

Drift ratio θ (%)	Buildings (n)	Left inadequate	Right inadequate	Any side inadequate	Both sides inadequate	Any side inadequate (%)	Both sides inadequate (%)	Median clearance ratio — adequate sides	Zero-gap share — inadequate sides (%)
0.3	174	28	29	38	19	21.8	10.9	63.5	100.0
0.5	174	28	29	38	19	21.8	10.9	38.1	100.0
0.75	174	28	29	38	19	21.8	10.9	25.4	100.0
1	174	28	29	38	19	21.8	10.9	19.1	100.0

Clearance ratio computed as available gap divided by s_{req} at each θ, reported for adequate sides only. Zero-gap share is the proportion of inadequate side instances with literally zero recorded clearance.

Among buildings meeting the threshold at θ = 1.0%, the smallest recorded gap is 0.40 m and the average is 2.00 m. All 57 inadequate buildings have zero recorded clearance. The two groups are completely non-overlapping, and no change in drift assumption would move any building from one category to the other. The inadequacy here is a layout problem, not a demand problem.

Figure 2 and Table 7 report ward-wise inadequacy at $\theta = 1.0\%$, which is representative of the full range because the counts do not vary across the tested values. Ward 2 shows the highest concentration of inadequate separation, with 47.4 percent of buildings failing on at least one side and 36.8 percent failing on both sides. Wards 42, 29, and 4 show intermediate levels of inadequacy, while Wards 5 and 22 show comparatively low levels.

Table 7
Ward level separation inadequacy for buildings with collapse probability greater than 0.3 (θ = 1.0%)

Ward	Buildings (n)	Any side inadequate (n)	Any side inadequate (%)	Both sides inadequate (n)	Both sides inadequate (%)
2	19	9	47.4	7	36.8
4	45	11	24.4	5	11.1
29	31	8	25.8	2	6.5
42	30	8	26.7	5	16.7
5	32	1	3.1	0	0
22	17	1	5.9	0	0

4.3 Interpretable Risk Profiling Using Regularised Logistic Regression

Regularised logistic regression was used to classify buildings into higher-risk and lower-risk categories using observable field and geometric attributes. Transparency and auditability were prioritised given the intended municipal application. The binary target classified a building as higher risk when either of two conditions was met: indicative damage grade ≥ 4, or joint geometric failure defined as debris exceedance at $\phi = 45^{\circ}$ or gap inadequacy at $\theta = 1.0\%$. The predictor set included building height, front setback, left setback, right setback, inter-building gap, floor area ratio (FAR), typology, and plinth-to-road level. In the full dataset, 352 buildings (31.8 percent) were classified as higher risk and 754 (68.2 percent) as lower risk.

Table 8 provides a detailed breakdown of the 352 higher-risk buildings by the condition(s) that triggered the flag. 145 buildings (41.3% of the higher risk group) are only structurally screened (damage grade ≥ 4 without joint geometric failure). 170 buildings (48.3%) are due to joint geometric failure alone (simultaneous debris exceedance and gap inadequacy, without damage grade ≥ 4). The other 37 buildings (10.5%) have both conditions occurring together. This disaggregation makes it clear what the model is predicting: no one path dominates the higher-risk flag. Geometric failure is about half of all higher risk classifications regardless of outcome of structural screening, and the other half are structural only cases. The 37 buildings that satisfy both conditions are the most constrained subset of the stock, combining structural vulnerability with inadequate clearance on both the debris and separation dimensions.

Table 8
Disaggregation of higher-risk buildings by triggering condition

Triggering Condition	Buildings (n)	Share of High Risk (%)	Share of Full Stock (%)
Structural only: damage grade ≥ 4, no joint geo failure	145	41.3	13.1
Joint geometric only: debris AND gap, no damage ≥ 4	170	48.3	15.4
Both structural and joint geometric	37	10.5	3.3
Total higher risk	352	100.0	31.8

Joint geometric failure is defined as simultaneous non-compliance with the prescribed minimum front setback (debris exceedance at φ = 45°) and inadequate inter-building gap (θ = 1.0%). Buildings triggering both conditions represent those where structural vulnerability and geometric clearance failure co-occur.

Model performance was evaluated using five-fold stratified cross-validation. Table 9 reports the fold-wise ROC AUC and F1 scores. The mean ROC AUC is 0.9164 $\pm$ 0.0143 and the mean F1 score is 0.8039 $\pm$ 0.0121, indicating strong discrimination and stable performance across folds. Figure 3 shows the same pattern graphically, with limited variation across folds and no sign of unstable performance in any single split. These results suggest that the model captures a consistent relationship between the observed predictors and the operational risk flag used in this study.

Table 9
Cross-validated ROC AUC and F1 scores across five folds.

Fold	ROC AUC	F1 Score
1	0.8968	0.7839
2	0.9365	0.8214
3	0.9289	0.8125
4	0.9148	0.8042
5	0.9050	0.7976
Mean ± SD	**0.9164 ± 0.0143**	**0.8039 ± 0.0121**

To improve probability reliability, Platt scaling was applied after fitting the base logistic model on the training data. The dataset was split into 80 percent training and 20 percent validation subsets. On the validation set, the calibrated model achieved ROC AUC = 0.9319 and F1 = 0.8421, which is consistent with the cross-validated estimates. Table 10 summarises the classification outcomes on the validation set. The model correctly classified 133 lower-risk cases and 64 higher-risk cases, with 10 false positives and 14 false negatives.

Table 10
Confusion matrix on validation set (N = 221)

Actual Low Risk	Predicted Low Risk	Predicted High Risk
	133	**10**
Actual High Risk	14	64

Figure 4 presents the same confusion matrix visually and shows that correct classifications clearly dominate both types of error. In operational terms, the false negatives are more consequential because they represent higher-risk buildings that remain unflagged, while false positives mainly reduce screening efficiency.

Figure 5 shows the calibration curve for the Platt-scaled model. The curve indicates reasonable agreement between predicted probabilities and observed event frequencies across the validation sample. This matters because the model is intended not only to classify buildings, but also to provide interpretable risk probabilities that can support prioritisation.

To identify the main drivers of prediction, permutation feature importance was computed on the validation set. Table 11 ranks the predictors by mean decrease in AUC after shuffling. Inter-building gap emerges as the strongest predictor, with a mean decrease in AUC of 0.0485. Plinth-to-road level ranks second at 0.0312, followed by building height at 0.0271 and FAR at 0.0158. Right and left setbacks contribute more modestly, while typology has the lowest measured importance in this dataset. This ranking indicates that immediate geometric and site-related conditions carry more predictive weight here than typology alone, even though structural system still remains part of the explanatory profile.

Table 11
Permutation feature importance ranked by mean decrease in AUC on validation set

Feature	Mean Decrease in AUC
Inter-Building-Gap	0.0485
Plinth to Road Level	0.0312
Building Height	0.0271
FAR	0.0158
Right Setback	0.0089
Left Setback	0.0067
Typology	0.0051

Figure 6 presents the partial dependence curves for the three most important predictors. The curve for inter-building gap shows a clear decline in predicted higher-risk probability as the minimum gap increases. The curve for plinth-to-road level indicates higher predicted risk where plinth elevation is low or negative relative to the road. The curve for building height rises steadily, showing greater predicted risk for taller structures. Together, these plots reinforce the main modelling result: within this dataset, higher-risk classification is driven most strongly by clearance, site condition, and height-related effects rather than by typology alone. The value of the model in this paper is therefore interpretive. It helps explain which observable field conditions are most closely associated with the combined screening-based risk flag.

4.4 Compliance Calculus and Compensatory Measures

The preceding analyses are now translated into compliance requirements and retrofit strategies. Building on the debris reach assessment, pounding risk evaluation, and risk profiling analysis, we develop prescriptive minimum setbacks and inter-building gaps by height class and structural typology (Table 12). We then quantify non-compliance across the surveyed stock and present a tiered framework of compensatory measures for buildings where geometry cannot be modified.

Minimum setbacks and inter-building gaps are derived from first-principles physics and validated against published research. Front setbacks are determined from debris reach calculations using the collapse angle family d = H · tan(φ). Side setbacks account for both debris spillover and lateral separation needed for pounding prevention. Inter-building gaps are estimated from drift-based separation demand using the formula $s_{req} = \Delta \square + \Delta \square$, where $\Delta = \theta \cdot H$ and θ ranges from 0.3% (serviceability) to 1.0% (near-yield).

Table 12
Prescriptive Minimum Setbacks and Gaps by Height Class and Typology

Height Class	Min Front Setback (m)	Min Side Setback (m)	Min Gap @ θ = 0.3% (m)	Min Gap @ θ = 1.0% (m)	Risk Level
≤ 6 m (1–2 storeys)	2.0	1.5–2.1	0.018–0.027	0.060–0.090	Moderate Risk
6–9 m (3 storeys)	2.5	1.5–2.1	0.045–0.068	0.150–0.225	High Risk
9–12 m (4 storeys)	3.0	1.5–2.1	0.063–0.095	0.210–0.315	High Risk
12–15 m (5 storeys)	3.5	1.5–2.1	0.081–0.121	0.270–0.405	High Risk
> 15 m (6 + storeys)	4.5	1.5–2.1	0.108–0.162	0.360–0.540	High Risk

Note: Front setbacks derived using φ = 45° (most probable collapse geometry). Side setback range (1.5–2.1 m) reflects structural typology: lower bound for C1/S types (modern concrete/steel); upper bound for U3/U4 (unreinforced masonry). Gap values derived from drift-based separation formula $(s_{req} = 2\theta H)$ at θ = 0.3% to 1.0%

4.4.1 Empirical Assessment of Current Stock

Non-compliance with prescriptive standards is assessed by comparing the 1,106 surveyed buildings against the height-dependent requirements in Table 13. Debris exceedance is determined by the 45-degree collapse angle, which represents the most probable failure geometry for the construction types observed. Pounding non-compliance is flagged when available inter-building gaps fall below the required separation at θ = 1.0% drift (near-yield condition). High-risk classification is assigned when either debris exceedance or gap inadequacy is detected, consistent with the joint-risk findings from Objective 3.

Table 13
Non-Compliance Rates for All 1,106 Buildings Against Height-Dependent Prescriptive Standards. Debris exceedance uses φ = 45°; pounding inadequacy uses θ = 1.0%.

Height Class	Buildings (n)	Share (%)	Debris Exceed φ = 45° (%)	Gap Inadequate θ = 1.0% (%)	High-Risk (%)
≤ 6 m	651	58.9	45.2	8.5	12.3
6–9 m	233	21.1	78.5	18.9	24.8
9–12 m	170	15.4	91.2	28.6	35.6
12–15 m	42	3.8	97.6	45.2	51.3
> 15 m	9	0.8	100.0	77.8	88.9
Total	1106	100.0	68.4	21.8	31.8

Current stock averages 2.15 m front offset and 1.35 m side setback, which exceeds prescriptive minima for heights up to 6 m but falls short for taller buildings. The sharp escalation in non-compliance beyond 9 m height reflects the linear relationship between height and debris reach ($d = H \cdot \tan \varphi$).

5 Discussion

The results reveal that seismic risk in Siliguri is not reducible to structural vulnerability alone. The geometry of dense urban development plays an equally important role. Across the surveyed stock, 68.4 percent of buildings exceed debris-safe setback at φ = 45°, 21.8 percent have inadequate inter-building separation at θ = 1.0%, and 31.8 percent fall into the combined higher-risk category. A substantial share of the built fabric may therefore compromise frontage safety and side clearance during strong shaking, even where total structural collapse does not occur. This supports the argument that seismic risk in dense urban areas must be treated as a building-to-street problem, not only as a building-level structural problem (Golla et al., 2022; Y. Hosseini et al., 2024; Yu & Gardoni, 2022). It also demonstrates that Rapid Visual Screening can be extended beyond conventional triage to produce planning-relevant indicators of debris encroachment and separation adequacy.

One of the clearest findings is that setback insufficiency is far more widespread than separation inadequacy. The two hazards are related but distinct, and the difference matters for how a municipality should respond to each. Debris exceedance rises sharply with height and becomes nearly universal among taller buildings. This is consistent with the geometric logic of the collapse-angle relation and with earlier work showing that falling facade elements and collapse debris can rapidly reduce usable carriageway width and block emergency access (Koren & Rus, 2019; Sediek et al., 2021; Yu & Gardoni, 2022). The separation analysis tells a different story. Inadequacy in the present stock is concentrated at zero or near-zero side clearance. It does not vary across the tested drift band from 0.3 percent to 1.0 percent. The clearance ratio diagnostic confirms this directly. Adequate sides carry a median clearance ratio of 19.1 at θ = 1.0%, meaning available gaps are on average nineteen times the near-yield demand. Every inadequate side instance, without exception, has zero recorded clearance. The two groups are completely non-overlapping. A municipality applying this framework does not need to resolve uncertainty about drift assumptions before acting on separation findings. The policy response of enforcing minimum side clearances and flagging zero-gap adjacencies in permit review is the same regardless of which drift threshold is assumed.

This finding does not contradict the pounding literature, which rightly emphasises dynamic properties, height mismatch, and soil interaction. Within a municipal screening context, however, the first-order problem in this stock is more fundamental: the physical absence of reserve space between adjacent buildings (Elwardany et al., 2025; Lin, 1996; Liu et al., 2022; Noman et al., 2016).

The paper does not attempt a full probabilistic blockage model or nonlinear structural simulation. Its contribution is more practical. A limited set of field-observable variables, collected through RVS, can be converted into debris and clearance indicators that are simple enough for local review yet grounded in established physical reasoning. The study therefore sits between two existing streams of work. One stream focuses on detailed structural or post-event debris modelling (Sediek et al., 2021; Yu & Gardoni, 2022). The other focuses on

network accessibility and resilience consequences after damage has already been estimated (El-Maissi et al., 2023; K. A. Hosseini & Hosseinioon, 2007). The present framework contributes a workable intermediate step for municipal practice. It does not replace either stream, but it bridges them at a screening level.

The regulatory implications are direct. The West Bengal Municipal (Building) Bye-Laws, 2007 specify front and side setbacks, but these values are often insufficient once building height increases beyond two storeys. Buildings above 9 m show debris exceedance rates above 90 percent at $\varphi = 45°$, while the tallest height class shows both near-universal debris exceedance and sharply rising gap inadequacy. A uniform setback rule is poorly suited to a stock that varies substantially in height and plot compactness. For much of the low-rise stock, the average front and side setbacks remain broadly comparable to the indicative minima proposed here. The problem intensifies as height and compactness increase. This aligns with the earlier literature gap on the weak translation of seismic reasoning into permit-review logic. Studies on pounding and debris have long established that geometry matters, yet local development control continues to treat setbacks as generic planning standards rather than as hazard-sensitive spatial margins (Cole et al., 2012). The findings support a height-sensitive setback framework as a direct empirical response to these observed patterns, not as a theoretical refinement.

The ground-coverage results tell the same story. Even under the primary reporting assumption, 39.5 percent of buildings exceed applicable coverage limits, and compliance declines with increasing plot size. Coverage, setbacks, and inter-building clearance are not separate issues in practice. They reflect the same spatial trade-off between built floor area and open safety margin. Where plot coverage rises, the residual space available for debris containment and lateral clearance narrows. Setback insufficiency is not an isolated design failure at individual plots. It is an accumulated outcome of densification, subdivision, and weak enforcement in small-plot urban settings (Golla et al., 2022; Sediek et al., 2021).

The risk model adds a further interpretive layer. Inter-building gap, plinth-to-road level, and building height emerge as the strongest predictors of higher-risk classification, while structural typology contributes comparatively less within this dataset. The disaggregation in Table 8 makes this concrete. Of the 352 higher-risk buildings, 170 (48.3 percent) are flagged by joint geometric failure alone, with no damage grade ≥ 4 trigger. Nearly half of all higher-risk buildings would be invisible to a purely structural screening approach. Equally, structural vulnerability and geometric constraint do not reliably coincide in this stock, with 145 buildings carrying structural flags but no geometric failure. Neither screening pathway alone captures the full higher-risk population. The joint flag is more informative than either component in isolation for municipal prioritisation purposes.

This does not suggest that structural typology is unimportant. The engineering literature clearly establishes otherwise. It suggests instead that within a screening framework based on field-observable variables, immediate geometric and site-related conditions may discriminate risk more sharply than typology alone. This is consistent with the operational emphasis of FEMA-style screening and with the practical motivation set out in the Introduction. RVS works best when it captures variables that are observable, comparable across wards, and directly linked to review decisions. Simple geometric variables carry substantial explanatory value when the modelling target is an operational risk flag rather than a structural damage state.

The study also speaks to how national seismic guidance is translated into local development control. The National Building Code provides the engineering basis for seismic design, but detailed setback and separation control is left to state and municipal regulations. The consequence is an uneven translation between structural principles and urban controls. The present findings indicate that this translation gap remains significant in high-risk, rapidly densifying cities. The indicative compliance framework proposed here should be read as an evidence-led starting point for regulatory revision, not as a final code prescription.

The method is most relevant to dense, rapidly urbanising cities with small plots, mixed building stock, and limited street-edge reserve space. In such settings, planning controls that appear adequate at low heights tend to become progressively insufficient as buildings rise and side margins shrink. The value of this paper lies in the method rather than in any single threshold value. The debris-reach logic, the drift-based separation screen, and the translation into compliance review can be adapted to other contexts. The specific values should, however, be tested against local building practices, bylaw traditions, and hazard conditions before direct transfer. Both debris behaviour and pounding risk are context-dependent (Cole et al., 2012; Liu et al., 2022).

These conclusions must be held alongside the study's limitations. The debris-reach analysis is a screening approximation. It does not simulate collapse mechanics, directional failure, or street-specific blockage propagation. The separation analysis is a simplified clearance check and not a full pounding model. Height was estimated as 3.0 m per storey where direct measurement was unavailable, and rear setbacks were not recorded in the field. The modelling target combines structural and geometric screening outcomes, which means the model should not be presented as a pure predictor of structural damage. The framework is intended to support early identification and municipal review. It demonstrates a replicable path from rapid field observation to interpretable seismic planning

indicators in a resource-constrained urban setting. Many municipalities lack the data or capacity for advanced modelling yet still need defensible methods to identify unsafe frontages and priority cases for further review. This framework is designed for that context.

6 Conclusions

The central question was whether field-observable building data can be translated into geometry-driven seismic risk indicators useful for municipal planning and permit review. The results confirm that it can, and that doing so reveals risk patterns that structural screening alone would miss.

Three findings stand out. First, Rapid Visual Screening can be extended beyond building-level damage triage to generate planning-relevant indicators of debris encroachment and side-clearance inadequacy. The collapse-angle and drift-based clearance checks used here are physically grounded, require no specialist modelling, and produce outputs that map directly onto existing regulatory categories of setbacks and inter-building gaps.

Second, the two geometry-driven hazards examined here behave differently and require different policy responses. Debris exceedance is primarily a height-scaling problem. It rises predictably with building height and calls for height-sensitive front setback standards in development control. Separation inadequacy, by contrast, is a binary clearance problem. It is driven entirely by the physical absence of gap between adjacent buildings, is insensitive to the assumed drift level across the full tested band, and points to a first-order enforcement problem rather than a demand-calibration problem. These two mechanisms require different regulatory responses and should not be treated as the same problem.

Third, the risk classification model demonstrates that geometric and site-related variables carry more discriminating power than structural typology alone within this dataset. Nearly half of all higher-risk buildings are flagged by joint geometric failure without any structural damage trigger. A screening approach that relies only on structural typology would leave this population unidentified.

These findings support a shift in how local development control treats setbacks and inter-building clearances. In seismically active, high-density cities where heights vary and plot reserves are narrow, these cannot be treated as generic planning standards. The indicative compliance framework proposed here offers a starting point for height-differentiated setback and gap requirements, and identifies compensatory measures for existing buildings where geometry cannot be changed.

The study has defined limitations. The debris-reach method is a screening approximation, not a collapse simulation. The separation analysis is a clearance check, not a full pounding model. The logistic regression uses a hybrid target that combines structural and geometric screening outcomes, and should not be read as a structural damage predictor. These constraints limit the precision of individual outputs but do not affect the validity of the method as a screening tool.

Future work should validate the debris-reach and separation thresholds against post-earthquake field observations, extend the framework to road-network blockage at the ward or corridor level, and test the compliance framework in other rapidly urbanising cities with similar plot morphology. The method is transferable. The thresholds require local calibration.

Declarations

Author Contribution

A.P.S.G wrote the main manuscript text and developed all the tables and figuresS.P.B and S.G. were involved supervision of the revision and have viewed the manuscript

References

1. Cole, G. L., Dhakal, R. P., & Turner, F. M. (2012). Building pounding damage observed in the 2011 Christchurch earthquake. *Earthquake Engineering & Structural Dynamics*, *41*(5), 893–913. https://doi.org/10.1002/eqe.1164
2. El-Maissi, A. M., Argyroudis, S. A., Kassem, M. M., & Mohamed Nazri, F. (2023). Integrated seismic vulnerability assessment of road network in complex built environment toward more resilient cities. *Sustainable Cities and Society*, *89*, 104363. https://doi.org/10.1016/j.scs.2022.104363
3. Elwardany, H., Mosa, B., Eldin Khedr, M. D., & Seleemah, A. (2025). Effect of earthquake induced-pounding on the response of a series of four adjacent buildings considering soil-structure interaction. *Structures*, *73*, 108382. https://doi.org/10.1016/j.istruc.2025.108382

4. FEMA. (2010). Debris Estimating Field Guide. *Federal Emergency Management Agency (FEMA)*, (September). https://www.fema.gov/pdf/government/grant/pa/fema_329_debris_estimating.pdf
5. FEMA 154. (2015). *Rapid Visual Screening of Buildings for Potential Seismic Hazards: Supporting Documentation*. https://www.fema.gov/media-library-data/1426210695613-d9a280e72b32872161efab26a602283b/FEMAP-155_508.pdf
6. Golla, A. P. S., Bhattacharya, S. P., & Gupta, S. (2020). The accessibility of urban neighborhoods when buildings collapse due to an earthquake. *Transportation Research Part D: Transport and Environment*, *86*, 102439. https://doi.org/https://doi.org/10.1016/j.trd.2020.102439
7. Golla, A. P. S., Bhattacharya, S. P., & Gupta, S. (2022). Assessing the discrete and systemic response of the Built Environment to an earthquake. *Sustainable Cities and Society*, *76*(September 2021), 103406. https://doi.org/10.1016/j.scs.2021.103406
8. Hong, H. P., Wang, S. S., & Hong, P. (2003). Critical building separation distance in reducing pounding risk under earthquake excitation. *Structural Safety*, *25*(3), 287–303. https://doi.org/10.1016/S0167-4730(02)00080-2
9. Hosseini, K. A., & Hosseinioon, S. (2007). *A Survey on the Parameters Affecting the Vulnerability of Urban Fabrics to Earthquake in Tehran*. *1*.
10. Hosseini, Y., Mohammadi, R. K., & Yang, T. Y. (2024). A comprehensive approach in post-earthquake blockage prediction of urban road network and emergency resilience optimization. *Reliability Engineering & System Safety*, *244*, 109887. https://doi.org/10.1016/j.ress.2023.109887
11. Kassem, M. M., Beddu, S., Ooi, J. H., Tan, C. G., Mohamad El-Maissi, A., & Mohamed Nazri, F. (2021). Assessment of Seismic Building Vulnerability Using Rapid Visual Screening Method through Web-Based Application for Malaysia. *Buildings*, *11*(10), 485. https://doi.org/10.3390/buildings11100485
12. Koren, D., & Rus, K. (2019). The Potential of Open Space for Enhancing Urban Seismic Resilience: A literature Review. *Sustainability*, *11*(21), 5942. https://doi.org/10.3390/su11215942
13. Koren, D., & Rus, K. (2025). Impact of earthquake-induced building debris on urban network functionality and citizen accessibility to urban functions. *Frontiers in Built Environment*, *11*. https://doi.org/10.3389/fbuil.2025.1602963
14. Lin, J.-H. (1996). Separation Distance to Avoid Seismic Pounding of Adjacent Buildings. *EARTHQUAKE ENGINEERING AND STRUCTURAL DYNAMICS*, *26*, 395403.
15. Liu, P., Fan, P.-P., Zhu, H.-X., & Yang, W.-G. (2022). A Seismic Pounding Risk-based Method for Determination of Minimum Separation Distance between Nonlinear Adjacent Buildings. *Journal of Earthquake Engineering*, *26*(15), 7855–7877. https://doi.org/10.1080/13632469.2021.1979133
16. Noman, M., Alam, B., fahad, M., Shahzada, K., & Kamal, M. (2016). Effects of pounding on adjacent buildings of varying heights during earthquake in Pakistan. *Cogent Engineering*, *3*(1), 1225878. https://doi.org/10.1080/23311916.2016.1225878
17. Sediek, O. A., El-Tawil, S., & McCormick, J. (2021). Seismic Debris Field for Collapsed RC Moment Resisting Frame Buildings. *Journal of Structural Engineering*, *147*(5). https://doi.org/10.1061/(ASCE)ST.1943-541X.0002985
18. Yu, Y.-C., & Gardoni, P. (2022). Predicting road blockage due to building damage following earthquakes. *Reliability Engineering & System Safety*, *219*, 108220. https://doi.org/10.1016/j.ress.2021.108220

Figures

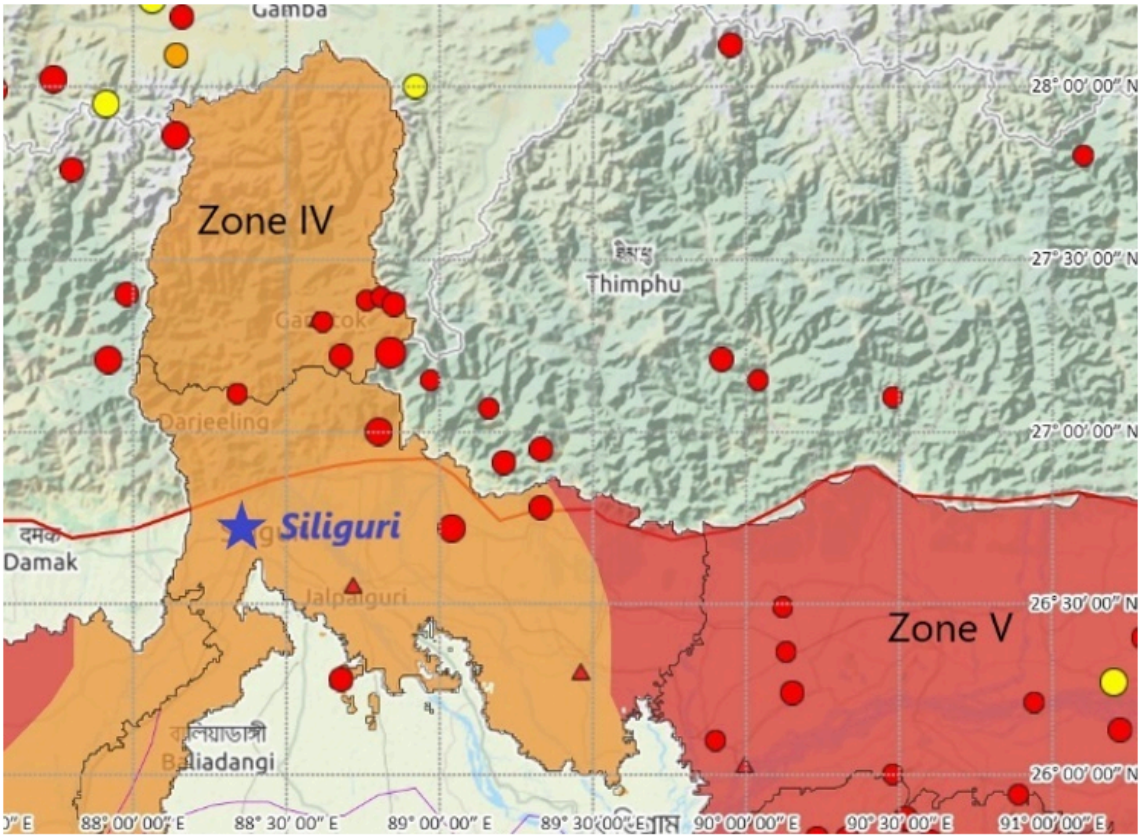


Figure 1

Location of SMC with respect to Seismic Zoning

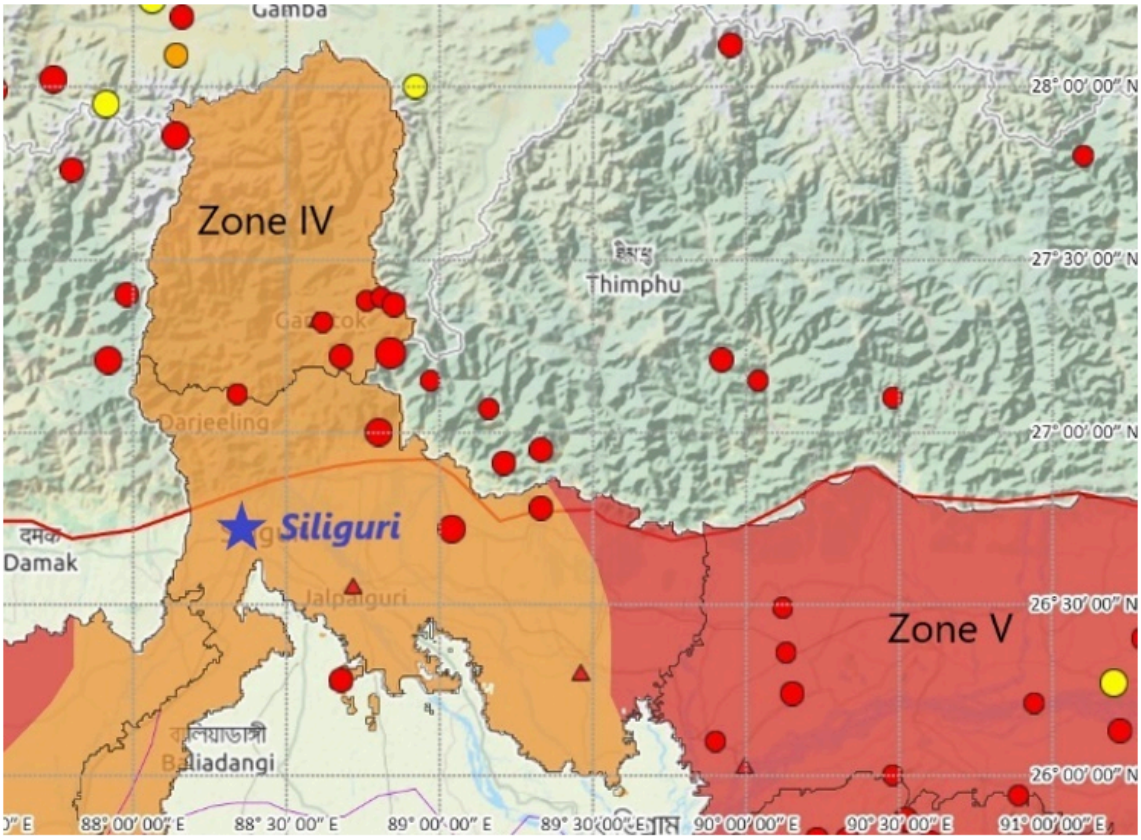


Figure 1

Location of SMC with respect to Seismic Zoning

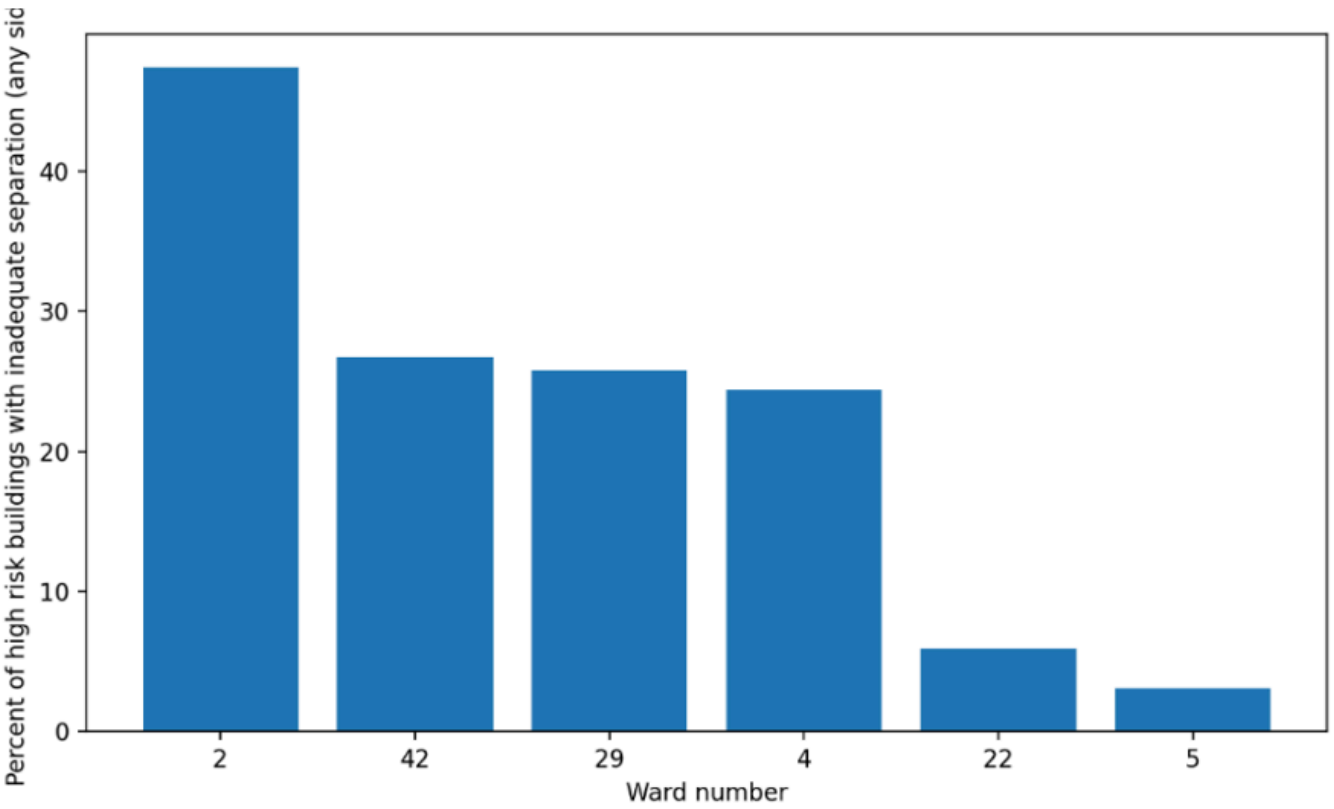


Figure 2

Share of high-risk buildings with inadequate separation by ward

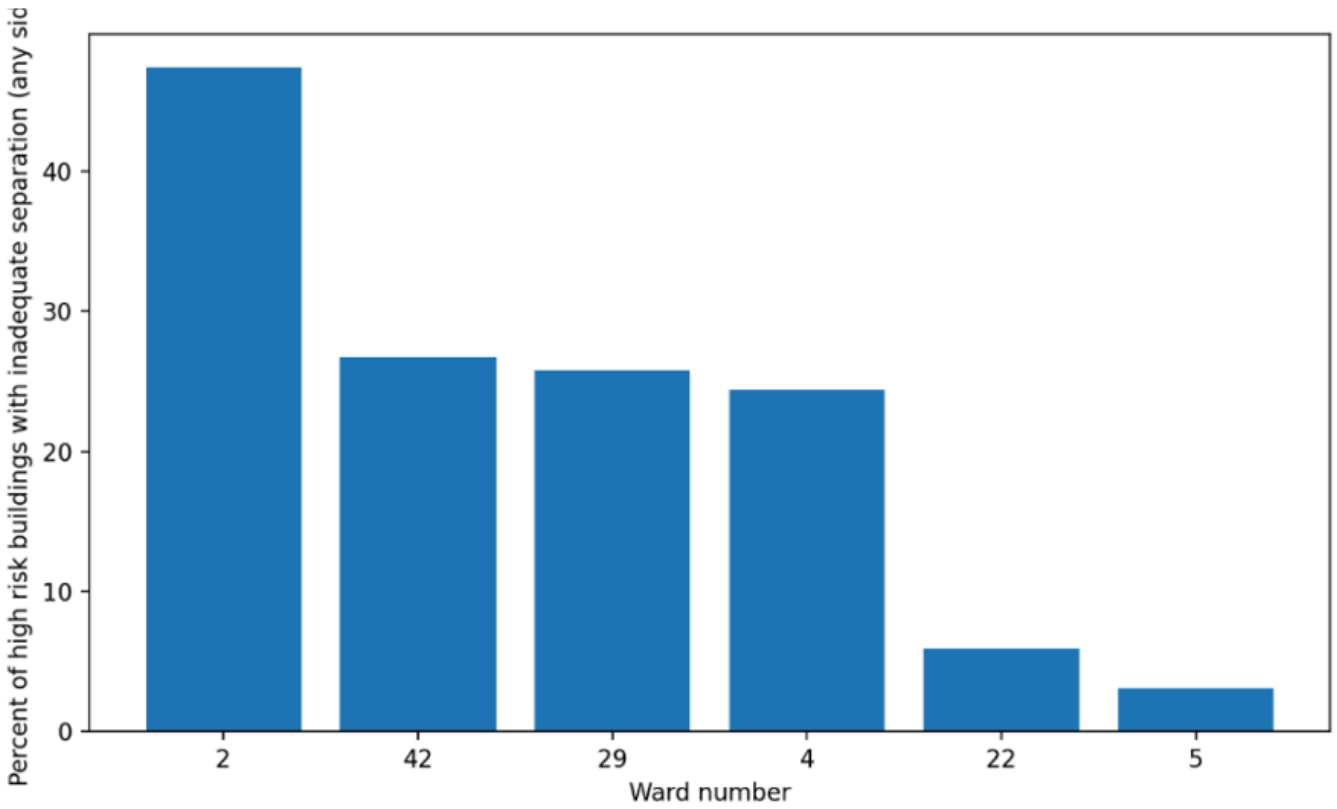


Figure 2

Share of high-risk buildings with inadequate separation by ward

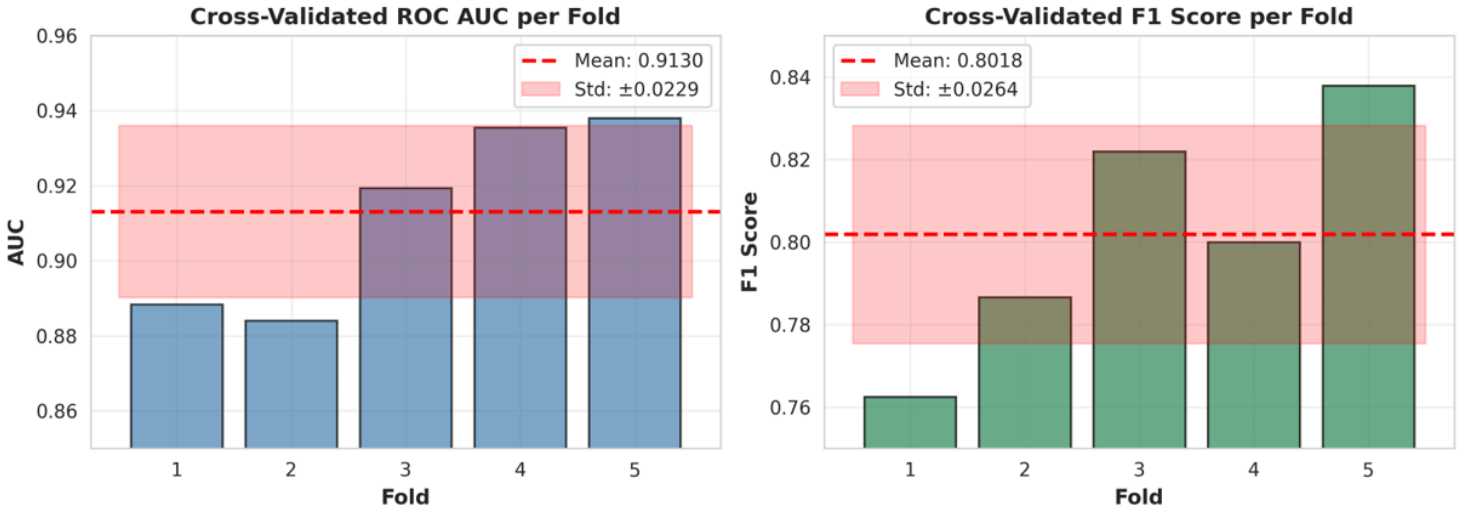


Figure 3

Cross-validated AUC and F1 by fold, with mean and standard deviation bands

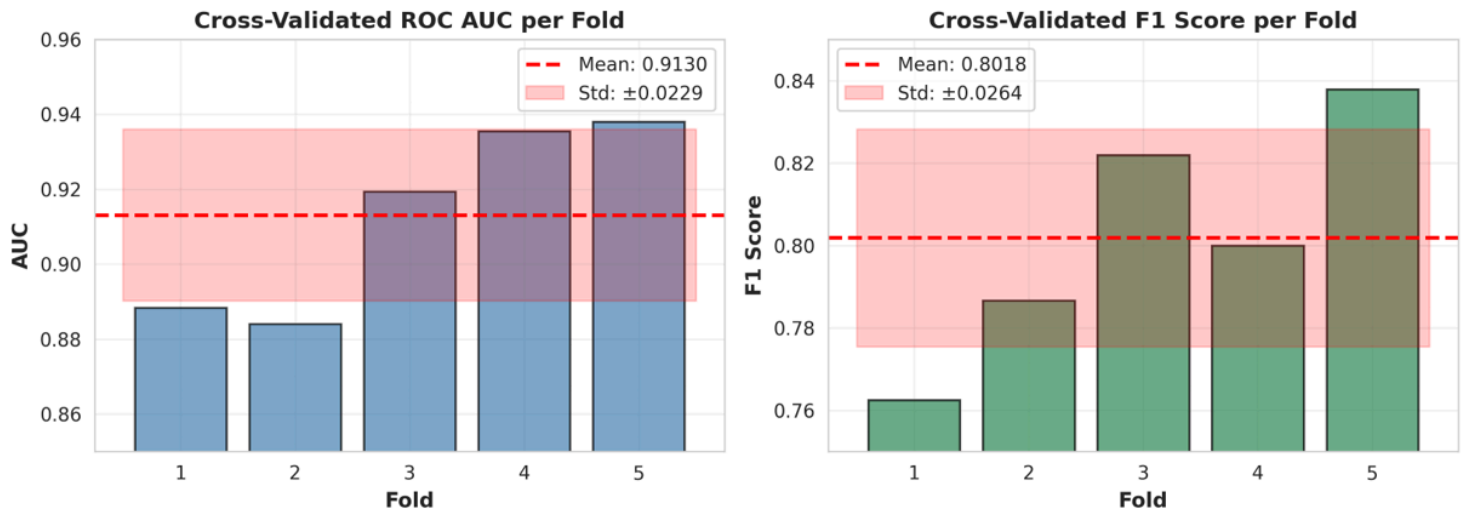


Figure 3

Cross-validated AUC and F1 by fold, with mean and standard deviation bands

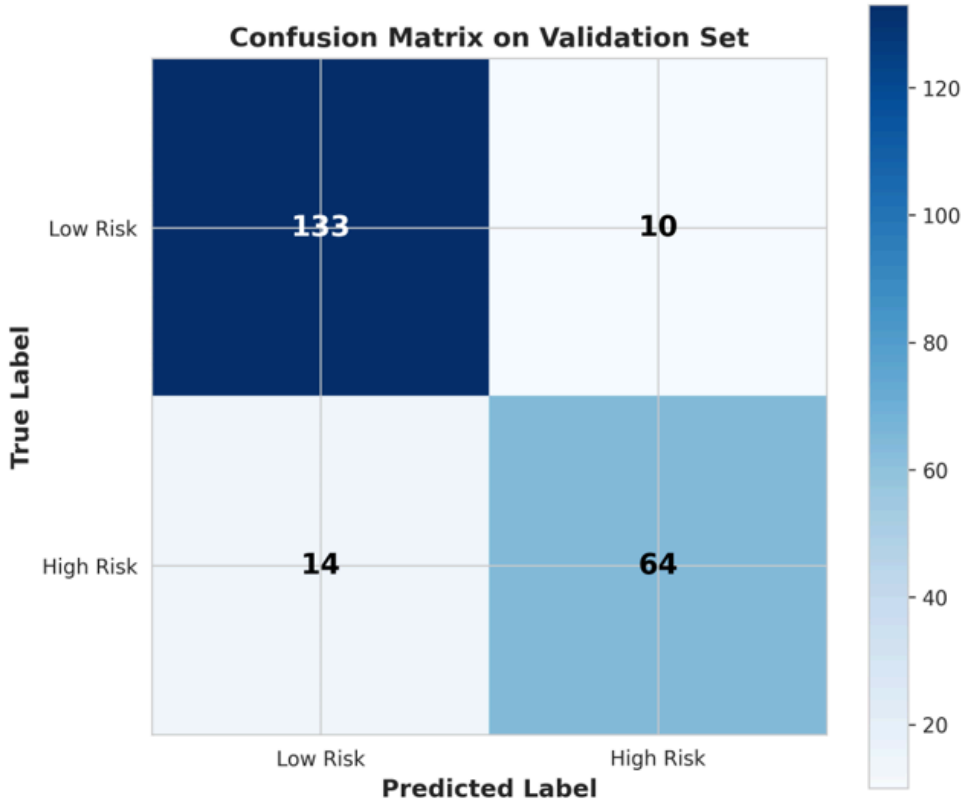


Figure 4

Confusion matrix visualization on validation set

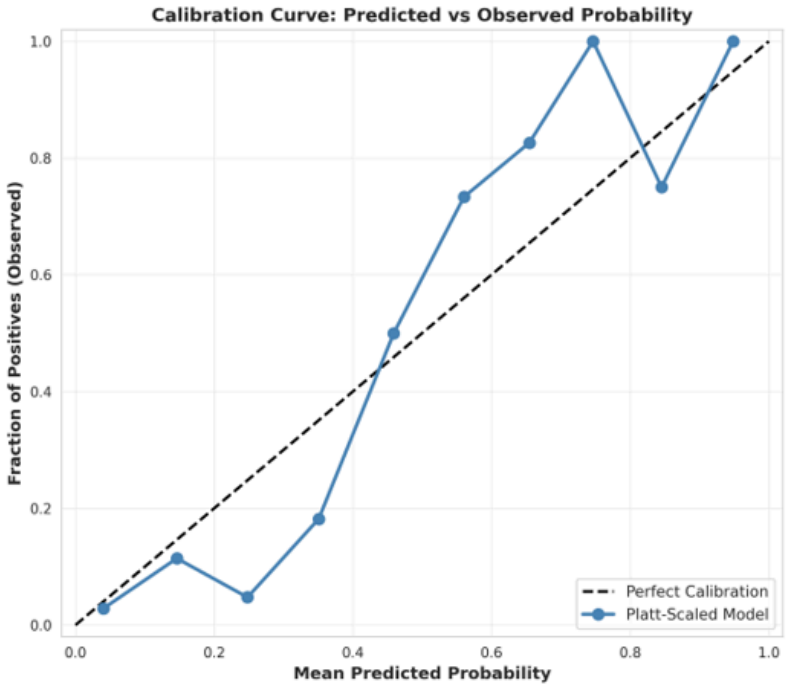


Figure 5

Calibration curve showing agreement between predicted and observed probabilities after Platt scaling.

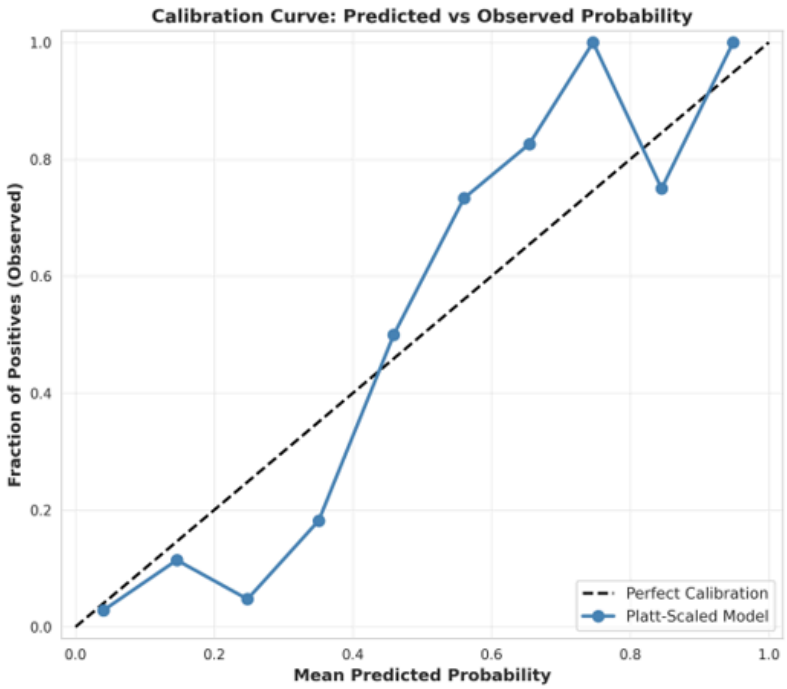


Figure 5

Calibration curve showing agreement between predicted and observed probabilities after Platt scaling.

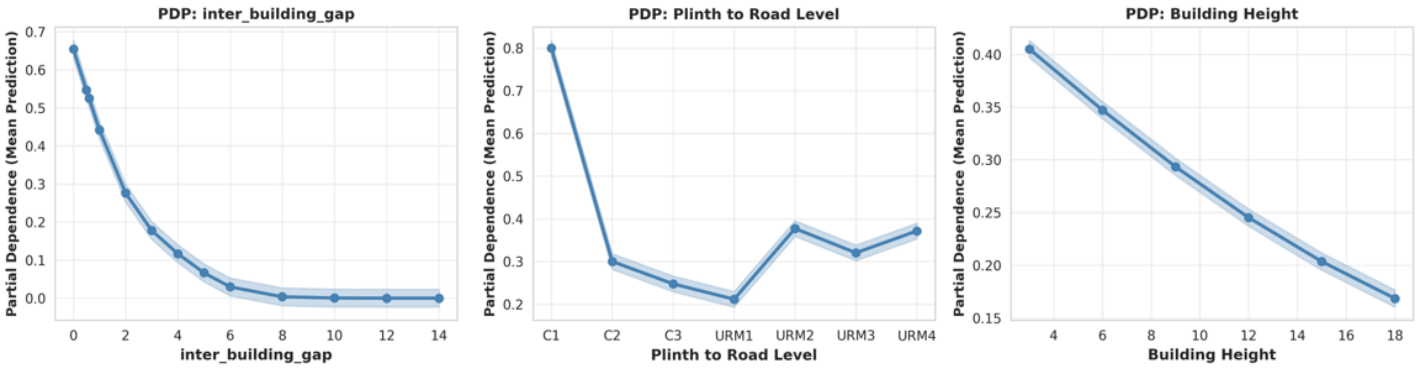


Figure 6

Partial dependence curves for the top three predictors: inter-building gap, plinth to road level, and building height. Each curve shows how the marginal predicted probability of high-risk changes with that feature.

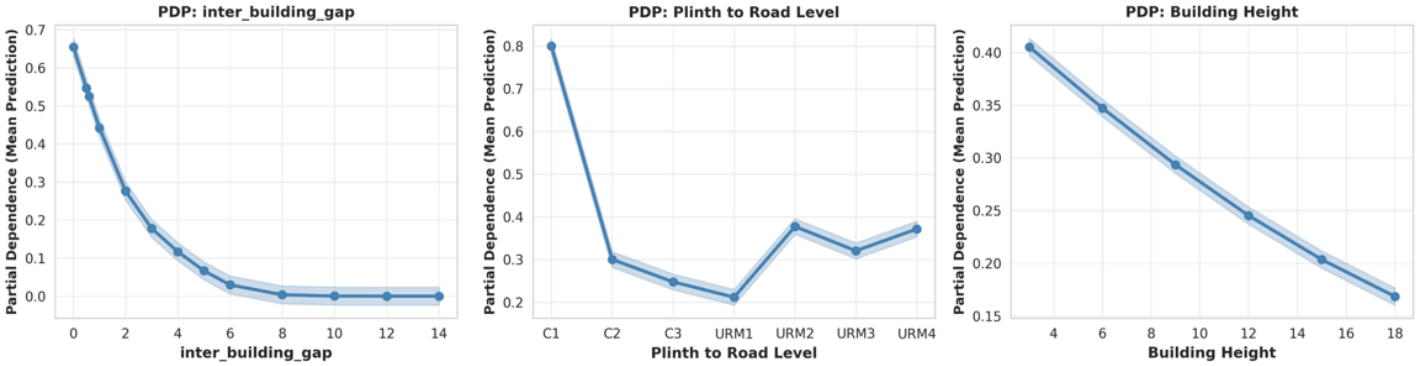


Figure 6

Partial dependence curves for the top three predictors: inter-building gap, plinth to road level, and building height. Each curve shows how the marginal predicted probability of high-risk changes with that feature.